Molecular Therapy
Nucleic Acids
Original Article

Antisense oligonucleotide-mediated exon 27 skipping restores dysferlin function in dysferlinopathy patient-derived muscle cells

Saeed Anwar,[1] Rohini Roy Roshmi,[1] Stanley Woo,[1] Umme Sabrina Haque,[2] Joshua James Arthur Lee,[1] William John Duddy,[3] Anne Bigot,[4] Rika Maruyama,[1] and Toshifumi Yokota[1,2,5]

[1]Department of Medical Genetics, Faculty of Medicine and Dentistry, University of Alberta, Edmonton, AB T6G 2H7, Canada; [2]Neuroscience and Mental Health Institute, Faculty of Medicine and Dentistry, University of Alberta, Edmonton, AB T6G 2R3, Canada; [3]Personalised Medicine Centre, School of Medicine, Ulster University, BT47 6SB Derry-Londonderry, UK; [4]Centre de Recherche en Myologie, Institut de Myologie, Sorbonne Université–L'Institut National de la Santé et de la Recherche Médicale (INSERM), 75651 Paris Cedex, France; [5]The Friends of Garrett Cumming Research and Muscular Dystrophy Canada Endowed Research Chair and the Henri M. Toupin Chair in Neurological Science, University of Alberta, Edmonton, AB T6G 2H7, Canada

Dysferlinopathies are debilitating autosomal recessive muscular dystrophies caused by mutations in the *DYSF* gene, encoding dysferlin, a protein crucial for sarcolemmal homeostasis and membrane resealing. Currently, no therapies exist for dysferlinopathies. Dysferlin features a modular structure with multiple calcium-dependent C2 lipid-binding domains. Clinical reports of mild, late-onset phenotypes suggest partial retention of functionality despite missing C2 domains, supporting exon-skipping therapies using antisense oligonucleotides (ASOs). In this study, we identified a patient-derived muscle cell line with a splice site mutation in *DYSF* intron 26, causing exon 26 exclusion, an out-of-frame transcript, and no detectable dysferlin protein. We hypothesized that skipping *DYSF* exon 27 could restore the reading frame and membrane repair function. Using an in-house *in silico* tool, we designed ASOs targeting exon 27. Treatment resulted in 65%–92% exon 27 skipping in myoblasts and myotubes, leading to a 39%–51% rescue of normal dysferlin expression, demonstrating robust efficacy of our designed ASOs. Two-photon laser-based assays indicated functional membrane repair. Additionally, we observed improved myotube fusion, cell vitality, and reduced apoptosis levels post-treatment. These findings provide proof of concept that *DYSF* exon 27 skipping restores functional dysferlin in patient-derived cells, paving the way for future *in vivo* and clinical studies.

INTRODUCTION

Dysferlinopathies are a genetically heterogeneous group of autosomal recessive muscular dystrophies, characterized by anomalous amyloid deposition and the presence of dysferlin fragments within skeletal muscle tissues.[1,2] With prevalence estimates ranging from 0.5 to 10/million, dysferlinopathies represent one of the most common forms of adult-onset muscular dystrophies.[3–5] The wide variability in prevalence is influenced by geographic and population factors, with higher rates in isolated ethnic groups due to consanguinity and founder mutations, while genetically diverse populations report lower rates.[6,7] Clinically, they manifest in multiple forms, including Miyoshi myopathy, limb-girdle muscular dystrophy recessive type 2 (LGMDR2, also known as limb-girdle muscular dystrophy type 2B or LGMD2B), distal myopathy with anterior tibial onset, dysferlin-deficient proximodistal phenotype, and dysferlin-associated asymptomatic hyperCKemia.[2,7–13] Onset typically occurs in adolescence or early adulthood, presenting significant difficulties (e.g., tiptoe standing, stair climbing).[7,13–16] While muscle weakness usually progresses slowly over the years, some rare cases report a rapid decline in mobility within approximately 5 years.[17]

Dysferlinopathies are caused by mutations in the *DYSF* (dystrophy-associated fer-1-like) gene located on chromosome 2p13.[2,8,18–20] This gene encodes dysferlin, a large (~237 kDa) modular protein that is crucial for skeletal muscle membrane repair.[1,2,21,22] Dysferlin predominantly localizes to the plasma membrane and is often observed in cytoplasmic vesicles associated with the t-tubule network.[19,20,23–25] It is ubiquitously expressed, with the highest abundance in skeletal and cardiac muscles.[7,26,27] Structurally, dysferlin comprises several functional domains, including seven lipid-responsive C2 domains, DysF domains, two Fer domains, and a transmembrane anchor.[7,28–33] These domains collaborate to maintain sarcolemmal homeostasis and facilitate plasma membrane resealing.[7] The DysF domain in particular is distinctive due to its nested structure, where the inner DysF domain is embedded within another DysF domain, likely as a result of evolutionary gene duplication events.[31,34,35] While the precise function of the DysF domains remains under investigation, they are considered crucial, as pathogenic mutations in these domains are frequently implicated in muscular dystrophies.[7,34,35] In general, variants in *DYSF* that lead to a complete

Received 16 August 2024; accepted 18 December 2024;
https://doi.org/10.1016/j.omtn.2024.102443.

Correspondence: Toshifumi Yokota, 8–31 Medical Sciences Building, University of Alberta, Edmonton, AB T6G 2H7, Canada
E-mail: toshifum@ualberta.ca

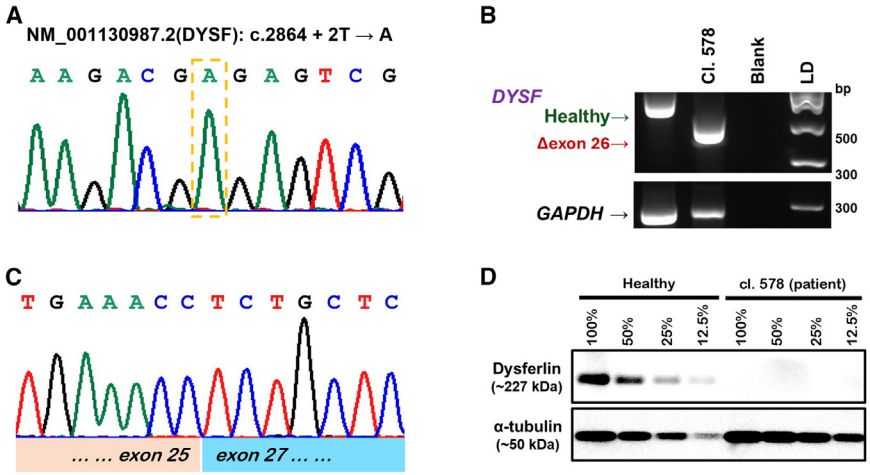

Figure 1. Dysferlinopathy patient cell line mutation analysis

(A) Sanger sequencing chromatogram for dysferlinopathy patient-derived myoblasts, showing a homozygous c.2864 + 2T → A mutation in the *DYSF* intron 26 splice donor site. (B) RT-PCR products separated on an agarose gel, indicating the absence of exon 26 in the cDNA synthesized from dysferlinopathy patient-derived myoblast RNA. (C) Sanger sequencing chromatogram for the RT-PCR products excised and purified from the agarose gels (B), confirming that the c.2864 + 2T → A mutation results in the exclusion of exon 26 from the transcript. (D) Immunoblot showing the absence of dysferlin protein in the patient-derived myoblasts compared to healthy controls, with α-tubulin as the loading control. LD, DNA ladder.

loss or functional impairment of dysferlin result in muscle degeneration, underscoring the critical importance of these domains.[1,2,8]

Unfortunately, there is currently no cure or effective treatment for dysferlinopathies.[7] However, reports of patients with very mild and late-onset phenotypes suggest that dysferlin lacking one or more of the repetitive C2 domains retains at least partial functionality.[36] This observation provides the rationale for developing exon-skipping therapies for dysferlinopathies. Exon-skipping therapy uses DNA-like synthetic molecules called antisense oligonucleotides (ASOs) to modulate pre-mRNA splicing, allowing exons harboring or near genetic mutations to be removed, thereby restoring the open reading frame.[37] This leads to the expression of an internally truncated but (at least) partially functional protein.

Previous investigations from our group and others have suggested that skipping single or multiple exons could offer a potential therapeutic strategy for dysferlinopathies.[38–42] In our prior work, we demonstrated that dysferlin-deficient patient-derived fibroblasts partially retained membrane resealing functionality when transfected with *DYSF* constructs lacking exons 26–27 or 28–29, producing an internally truncated dysferlin protein.[41] This suggests that certain *DYSF* exons may be dispensable for essential protein functions (e.g., membrane repair). Exon pairs 26–27 and 28–29 specifically code for parts of the DysF domain, a region implicated in muscular dystrophies due to its frequent mutation, although its precise functional role is still under investigation.[7,31,34,43] Targeting these regions for exon-skipping therapies could address a broad spectrum of mutations within this domain. Building on this foundation, the present study aimed to test the hypothesis that skipping exon 27 in dysferlinopathy patient-derived muscle cells, which lack exon 26, could restore the reading frame of *DYSF* and potentially recover functional dysferlin protein.[41] We designed exon-skipping ASOs targeting exon 27 and tested their efficacy *in vitro*. Using a battery of *in vitro* molecular techniques, we demonstrated that treatment with our designed ASOs significantly rescued dysferlin expression and, importantly, that the expressed proteins were functional. Our results lay the groundwork for future *in vivo* studies and the potential clinical translation of exon-skipping therapies for dysferlinopathies amenable to *DYSF* exon 27 skipping.

RESULTS

Mutation analysis confirms pathogenic exon 26 splice site mutation

We first assessed the mutation status in a dysferlinopathy patient-derived immortalized myoblast, cl.578. Sanger sequencing confirmed the presence of a homozygous splice site mutation, c.2864 + 2T → A, at the 5′ splice donor site of intron 26–27 in the *DYSF* gene of the patient-derived cell line (Figure 1A). This mutation, documented in the ClinVar database (rs1553553943, accession no.: VCV000498750.4), is classified as pathogenic. The alteration disrupts the canonical splice donor site, leading to the exclusion of exon 26 in the cDNA, as observed by RT-PCR and Sanger sequencing of the RT-PCR product (Figures 1B and 1C). Subsequent western blotting showed no expression of dysferlin protein by the cells. Analysis of the *DYSF* transcript revealed that exon 26 exclusion causes a frameshift in its reading frame (Figure S1). To restore the reading frame would involve the skipping of exon 27. The resultant reading frame, lacking both exons 26 and 27, would maintain an in-frame transcript, potentially producing an internally truncated but (at least partially) functional dysferlin protein.

ASOs efficiently skip exon 27 and restore dysferlin protein expression

Based on our hypothesis, we designed ASOs to remove exon 27 and restore the reading frame. Using an in-house-developed computational tool, we designed three ASOs, namely DYSF1, DYSF2, and DYSF3, intended for therapeutic exon 27 skipping (Figure 2A).[44,45] These ASOs were then synthesized using phosphorodiamidate morpholino oligomer (PMO) chemistry from a commercial vendor (GeneTools, Philomath, OR). The ASOs were transfected into patient-derived myoblasts and differentiated myotubes at a 10-μM dose with the aid of 6.0 μM EndoPorter (a weak-base amphiphilic peptide-based transfection reagent commercially available for PMO transfection; GeneTools) (Figure 2B). RT-PCR analysis 48 h

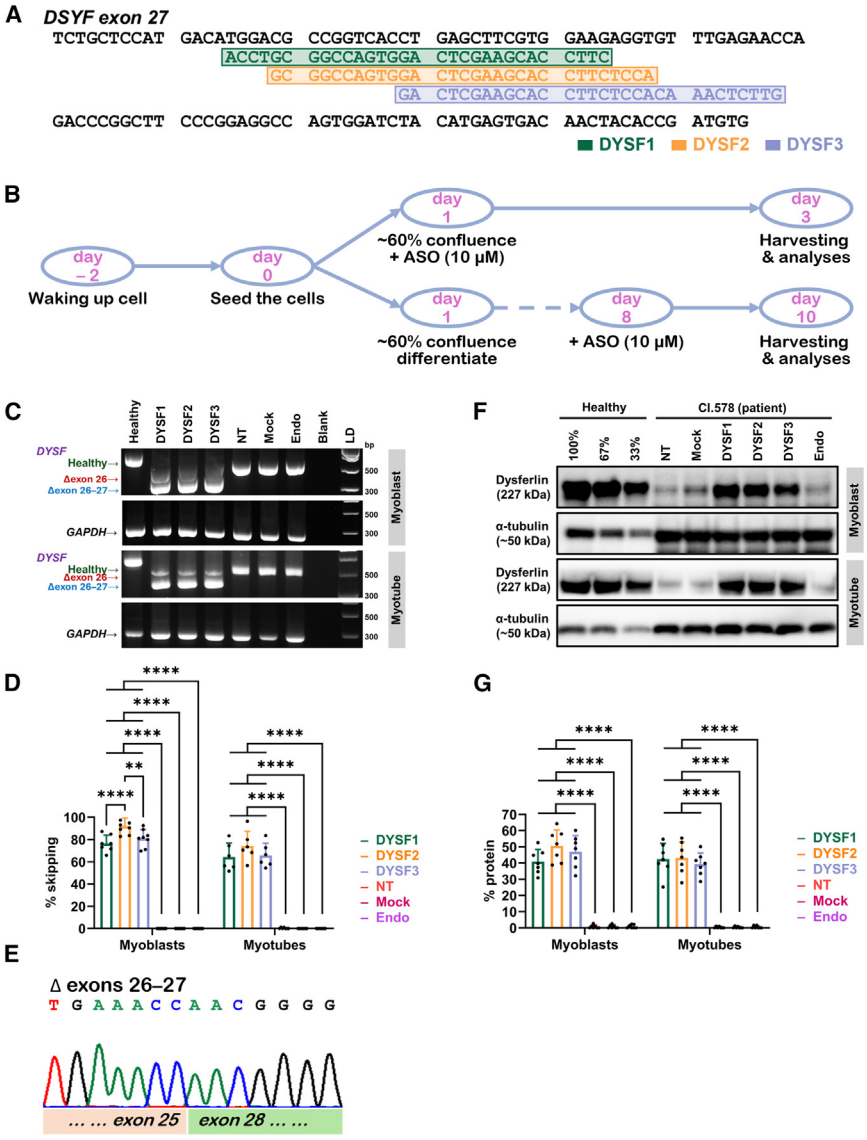

Figure 2. Efficiency of ASO-mediated exon 27 skipping and dysferlin protein restoration

(A) Sequence and target regions of the ASOs we designed for exon 27 skipping. (B) Schematic diagram showing the experimental design for ASO treatment in patient-derived myoblasts and myotubes. Cells were treated with ASOs at 10 μM dose either when they reached ~60% confluence (myoblasts) or after 7 days of differentiation into myotubes. Cells were harvested and analyzed 48 h post-treatment. (C) Representative image showing RT-PCR products separated on an agarose gel, indicating the skipping of exon 27 in patient-derived myoblasts and differentiated myotubes. (D) Skipping efficiency of the ASOs in both myoblasts and myotubes as determined by densitometric analysis of the RT-PCR products from agarose gel images (C). (E) Sanger sequencing chromatogram for the RT-PCR products excised and purified from the agarose gels in (C), confirming that ASO treatment results in the skipping of exon 27 from the transcript. (F) Representative image showing immunoblot suggesting the restoration of dysferlin protein in patient-derived myoblasts and differentiated myotubes post-treatment with ASOs, with α-tubulin as the loading control. (G) Percentage of protein restoration compared to normal (healthy) level post-treatment with ASOs in both myoblasts and differentiated myotubes as determined by densitometric analysis of the immunoblot images obtained from immunoblotting experiments (F). Statistics, one-way ANOVA with Tukey's multiple comparisons test; $^{*}p < 0.05$; $^{**}p < 0.01$; $^{***}p < 0.001$; $^{****}p < 0.0001$. Data are represented as mean ± standard deviation. NT, non-treated; Endo, EndoPorter.

post-treatment showed efficient skipping of *DYSF* exon 27 in both myoblasts and differentiated myotubes (Figure 2C). The ASOs achieved 78.5% (±9.58) skipping efficiency in myoblasts, with DYSF2 being the most effective (87.04% ± 6.84%) (Figure 2D). In differentiated myotubes, the ASOs achieved 63.16% (±12.2) skipping efficiency, with DYSF2 again performing the best (70.05% ± 13.07%) (Figure 2D). Sanger sequencing of the RT-PCR product confirmed the efficient skipping of *DYSF* exon 27 (Figures 2E and S2).

To assess dysferlin protein rescue, we performed western blotting analysis and found that patient-derived cells treated with the ASOs expressed significant amounts of dysferlin protein (Figure 2F). Our designed ASOs rescued 46.19% ± 9.35% of normal dysferlin levels in myoblasts and 41.62% ± 8.45% in differentiated myotubes (Figure 2G). DYSF2 showed the highest protein rescue potential, achieving 50.64% ± 10.39% in myoblasts and 43.19% ± 9.08% in differentiated myotubes, although there was no statistically significant difference from DYSF1 and DYSF3 (Figure 2G). We observed a residual level of dysferlin protein expression up to 7 days post-treatment, with 9.04% ± 3.22% of normal dysferlin levels still detectable (Figure S3). Cells treated with DYSF2 retained the highest residual protein expression, at 9.66% ± 3.43% of normal levels, although this was not significantly different from DYSF1 and DYSF3. However, by 14 days post-treatment, dysferlin expression levels were no longer detectable in these cells. These results demonstrate that the ASOs we designed were efficient in therapeutically skipping exon 27 and rescuing dysferlin protein expression.

Functional dysferlin protein rescues plasma-membrane resealing

Dysferlin is known to play a critical role in facilitating cell membrane repair, and dysferlin-deficient cells fail to reseal membrane injuries efficiently.[46,47] To determine whether the expressed proteins post-treatment with ASOs were functional, we performed a laser wounding assay.[48,49] This assay tested the ability of treated cells to heal wounds induced by a two-photon laser. All three designed ASOs significantly

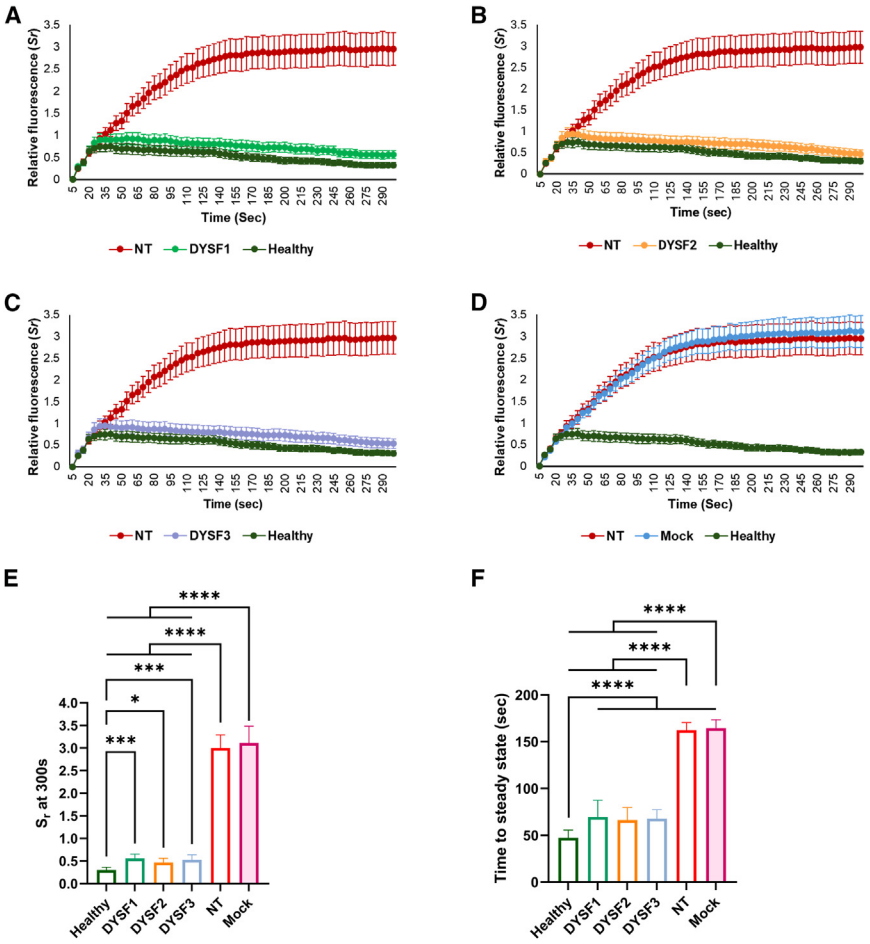

Figure 3. Laser wounding assay assessing membrane resealing performance in dysferlinopathy patient-derived myoblasts post-ASO treatment

(A–D) Relative fluorescence intensity (S_r) over time for dysferlinopathy patient-derived myoblasts treated with ASOs—for example, DYSF1 (A), DYSF2 (B), DYSF3 (C), and mock (D) compared to NT and healthy controls. The graphs show changes in fluorescence at the ablation site induced by a two-photon laser, indicating the membrane resealing capacity of the cells. (E) Quantification of S_r at 300 s (endpoint) post-wounding, demonstrating the membrane resealing efficiency of ASO-treated cells compared to non-treated and mock-treated cells. (F) Time to reach a steady-state S_r post-wounding for ASO-treated, non-treated, mock-treated, and healthy control cells. Shorter times indicate more efficient membrane resealing. One-way ANOVA with Tukey's multiple comparisons test; $^{*}p < 0.05$; $^{**}p < 0.01$; $^{***}p < 0.001$; $^{****}p < 0.0001$. Data are represented as mean ± standard deviation.

rescued plasma membrane resealing in myoblasts, as measured by changes in relative fluorescence intensity (S_r) over time (Figures 3A–3D). The S_r value at the endpoint of the laser wounding assay was significantly lower in ASO-treated cells compared to non-treated cells ($p < 0.0001$) (Figure 3E). Additionally, the time to reseal the membrane post-injury was significantly reduced in ASO-treated cells, as indicated by the time to achieve a steady state in S_r ($p < 0.0001$) (Figure 3F). Although there was a significant difference in both the S_r value at the endpoint ($p < 0.001$, healthy vs. DYSF1 and DYSF3; $p < 0.05$, healthy vs. DYSF2) and the time required to reach steady state ($p < 0.0001$) between the ASO-treated cells and healthy controls, the values for the treated cells were closer to those of healthy controls compared to non-treated and mock-treated cells ($p < 0.0001$) (Figures 3E and 3F). These results suggest that the dysferlin protein expressed post-treatment was indeed functional and capable of efficiently facilitating membrane repair.

ASO treatment enhances myogenic fusion in patient-derived cells

Dysferlin deficiency has been reported to impair the differentiation of myoblasts into myotubes, resulting in the improper development of multinucleated myofibers, a hallmark of dysferlinopathy.[50,51] We assessed the effect of our designed ASOs on myogenic fusion in patient-derived cells (Figure 4A). The myogenic fusion index (MFI) was significantly lower in patient-derived muscle cells (MFI: 22.82 ± 12.31) compared to healthy controls (MFI: 49.18 ± 12.82) (Figures 4A and 4B). ASO treatment significantly enhanced the MFI in patient-derived muscle cells differentiated into myotubes, with a post-treatment MFI of 37.12 ± 12.49 (Figure 4B). Specifically, we observed an ∼65% increase in MFI in cells treated with DYSF1 (MFI: 37.7 ± 12.31) and DYSF3 (MFI: 37.74 ± 13.04), indicating substantial improvement in myogenic fusion.

Following this, we examined the expression of two myogenic differentiation proteins—myogenin and myomaker—in these cells (Figure S4). Both proteins were significantly elevated in patient-derived cells compared to healthy cells, and ASO treatment did not significantly affect the expression levels of these proteins. We also evaluated caveolin 3, a dysferlin-binding protein involved in membrane repair. Caveolin 3 levels were reduced in patient-derived cells relative to controls, and although ASO treatment caused a modest increase, this change was not statistically significant (Figure S4).

ASO treatment reduces cytotoxicity and apoptosis while improving cell vitality

Assessing cytotoxicity, vitality, and apoptosis post-treatment is crucial for evaluating the efficacy and safety of any therapeutic strategy.[52,53] We used a fluorescence/luminescence-based triplex assay, ApoToxGlo, to simultaneously assess these parameters in

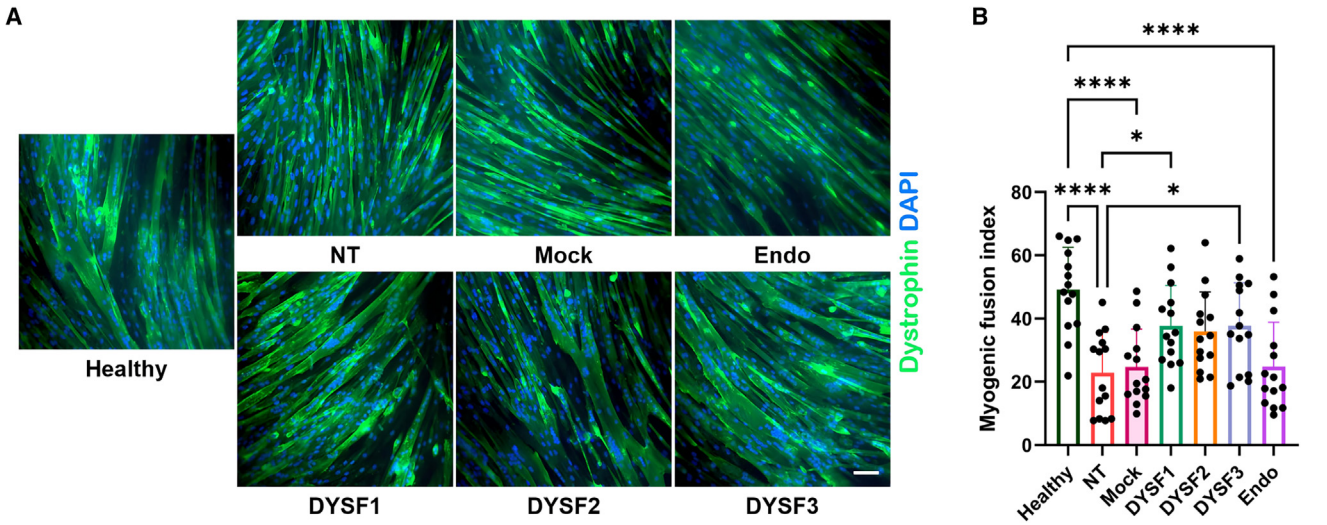

Figure 4. Effect of ASO treatment on myogenic fusion in dysferlinopathy patient-derived muscle cells

(A) Immunocytochemistry images of myotubes stained for dystrophin (green) and nuclei counterstained with DAPI (blue). The images compare healthy control myotubes, NT patient-derived myotubes, mock-treated myotubes, Endo-treated myotubes, and myotubes treated with ASOs (e.g., DYSF1, DYSF2, DYSF3). (B) Quantification of the myogenic fusion index (MFI) for healthy control myotubes, NT, mock-treated, Endo-treated, and ASO-treated myotubes. The MFI is calculated as the number of nuclei in myotubes (defined as cells with at least two nuclei sharing the same cytoplasm). Scale bar, 100 μm. One-way ANOVA with Tukey's multiple comparisons test; *$p < 0.05$; **$p < 0.01$; ***$p < 0.001$; ****$p < 0.0001$. Data are represented as mean ± standard deviation.

patient-derived cells at different time points post-treatment (Promega, Madison, Wi). This assay measures cell viability, compound cytotoxicity, and caspase-3/7 activity (indicative of apoptosis induction) in the same cell culture well.

Patient-derived myoblasts showed increased compound cytotoxicity at 24 and 48 h post-treatment, with slightly reduced signals in ASO-treated cells, indicating a reduction in cytotoxic effects (Figure 5A). The vitality of patient-derived myoblasts decreased over time; however, ASO treatment significantly improved vitality at 24 and 48 h post-treatment compared to non-treated cells (Figure 5B). Apoptosis, measured by caspase 3/7 activity, was higher in patient-derived cells compared to healthy controls at all time points (Figure 5C). Treatment with ASOs resulted in a significant reduction in caspase 3/7 activity, indicating decreased apoptosis. These findings suggest that ASO treatment not only reduces cytotoxicity and apoptosis but also enhances cell vitality in patient-derived myoblasts.

Overall, these results underscore the potential therapeutic gains, cell-level safety, and functional benefits of ASO-mediated exon 27 skipping, supporting its clinical feasibility for treating dysferlinopathy patients.

DISCUSSION

This study presents compelling evidence that ASO-mediated exon 27 skipping in *DYSF* effectively restores functional dysferlin protein in dysferlinopathy patient-derived cells. Our findings demonstrate significant exon 27 skipping efficiency, robust rescue of functional dysferlin, as evidenced by the presence of the protein on western blots, enhanced membrane resealing, and myogenic fusion capabilities. Moreover, ASO treatment reduced cytotoxicity and apoptosis while improving cell vitality, highlighting the therapeutic potential and cell-level safety of this approach.

Few reports are available on dysferlin exon skipping in patient-derived cell cultures.[38–42,54] Most studies on exon-skipping therapies for dysferlinopathies have focused on exon 32 skipping due to its association with a mild phenotype resulting from the in-frame deletion of exon 32.[36,38,40] Previous research demonstrated that *DYSF* exon 32 skipping increases dysferlin expression and restores membrane healing deficits *in vitro* using wound healing and osmotic shock assays.[38] Additionally, in cultured cells from a patient with an intronic mutation that activated the inclusion of a pseudoexon in dysferlin transcripts, ASO treatment resulted in skipping the pseudoexon and producing a considerable level of wild-type dysferlin.[42] Further studies have shown the feasibility of skipping various in-frame dysferlin exons—for example, exons 8, 9, 19, 25, 30, 21, 29, 30, 34, and 38—using RT-PCR and western blots, although the functional benefits *in vitro* remain unclear.[39,40] Previous reports from our group demonstrated that skipping *DYSF* exons 28–29 in patient-derived fibroblasts with a missense mutation in exon 28 rescued membrane-sealing ability.[41] Verwey et al. also indicated the feasibility of exon 29 skipping in dysferlinopathy patient-derived muscle cells lacking exon 28.[40] Building on these findings, the present study targeted exon 27, a novel approach for dysferlinopathies. We showed that exon 27 skipping in patient-derived myoblasts lacking exon 26 can restore dysferlin function, suggesting broader applicability for patients with dysferlinopathies who could be treated with exon-skipping therapies.

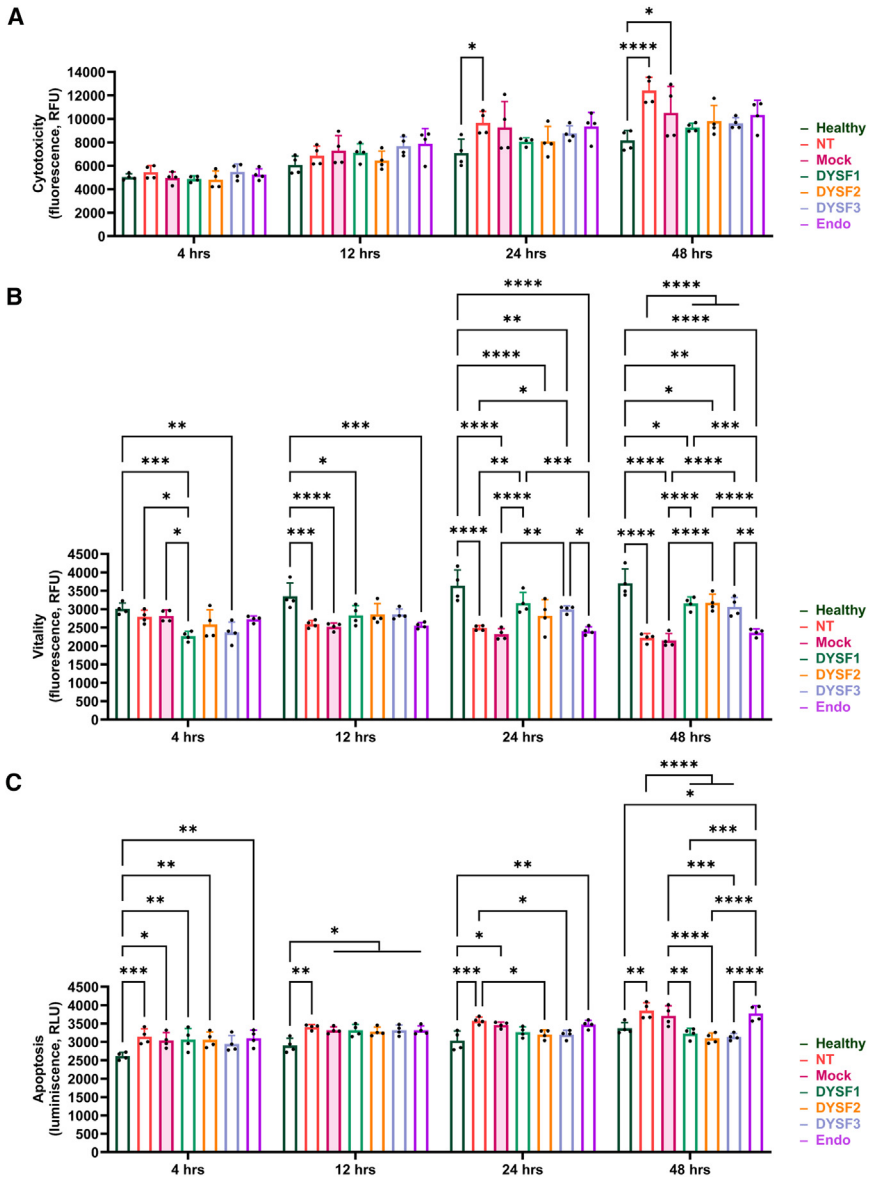

Figure 5. Evaluation of cytotoxicity, cell viability, and apoptosis in dysferlinopathy patient-derived myoblasts post-ASO treatment

(A) Cytotoxicity assessment in healthy control, NT, mock-treated, Endo-treated, and ASO-treated (DYSF1, DYSF2, DYSF3) myoblasts at 4, 12, 24, and 48 h post-treatment. Cytotoxicity is measured as relative fluorescence units (RFU), with higher values indicating increased cytotoxicity. (B) Cell vitality assessment in healthy control, NT, mock-treated, Endo-treated, and ASO-treated myoblasts at 4, 12, 24, and 48 h post-treatment. Viability is measured as RFU, with higher values indicating greater cell viability. (C) Apoptosis assessment in healthy control, NT, mock-treated, Endo-treated, and ASO-treated myoblasts at 4, 12, 24, and 48 h post-treatment. Apoptosis is measured as relative luminescence units (RLU), with higher values indicating increased apoptosis. One-way ANOVA with Tukey's multiple comparisons test; $^{*}p < 0.05$; $^{**}p < 0.01$; $^{***}p < 0.001$; $^{****}p < 0.0001$. Data are represented as mean ± standard deviation.

This study is novel in several respects. It is the first to demonstrate the efficacy of exon 27 skipping in restoring functional dysferlin protein in dysferlinopathy patient-derived cells. Using an in-house-developed computational tool, we designed highly efficient exon-skipping ASOs, achieving substantial exon 27 skipping and significant dysferlin protein rescue (Figure 2). The success of our ASOs underscores the value of computational tools for optimizing and enhancing the efficacy of exon-skipping strategies.[45,55] Our findings show that exon 27 skipping confers therapeutic benefits by improving membrane resealing capacity, a critical function compromised in dysferlinopathies (Figure 3). Additionally, treatment with these ASOs enhanced myogenic differentiation and improved cell viability, which are essential for maintaining healthy muscle function (Figures 4 and 5). Notably, the impact of exon skipping on *in vitro* myogenic fusion in patient-derived muscle cells has been largely unexplored in the context of dysferlinopathies. Moreover, the effects of ASO therapy on cytotoxicity, cell vitality, and apoptosis in dysferlinopathy patient-derived cells have not been previously reported (Figure 5). Overall, this simple yet comprehensive approach provides a thorough *in vitro* evaluation of the therapeutic potential and mechanistic insights of *DYSF* exon 27 skipping.

The modular structure of dysferlin, with its multiple calcium-dependent C2 lipid-binding domains, enables partial functionality even when some domains are absent.[7,39] Among the DYSF exons previously shown to be feasible targets for exon skipping using ASOs, exons 8, 9, 34, and 38 encode parts of the C2 domains, while exon 25 codes for part of the FerB domain, and the specific role of exon 19 remains unclear.[7] Exons 29 and 30, along with exons 26 and 27, encode regions of the DysF domain. Our findings that muscle cells lacking exons 26 and 27 still exhibit functional dysferlin suggest that the DysF domains may not be essential for plasma membrane resealing, or their function may be compensated by other domains. This raises intriguing questions about the specific roles of DysF domains in muscle physiology and their dispensability, which could have broader implications for designing exon-skipping strategies that target multiple exons without compromising overall protein function. This also indicates that DysF domains, similarly to the C2 lipid-binding domains, can be dispensable. Together with the outcomes of our prior study, we demonstrate that both exon pairs 26–27 and 28–29 are dispensable, and the resulting internally truncated

protein remains (at least) partially functional. These insights could inform the design of more targeted exon-skipping strategies that preserve essential functions while bypassing pathogenic mutations. In particular, investigating the effect of skipping exons 26–29 entirely would be an interesting future direction. Notably, some recent cohort studies identified the DysF domain of *DYSF* as a mutational hotspot, making it a target for multi-exon-skipping therapy with wider applicability to patients with dysferlinopathy.[43,56]

Our study highlights the therapeutic promise of ASO-mediated exon 27 skipping for dysferlinopathy patients. We demonstrate that the ASO therapy we designed reduces cytotoxicity and apoptosis in patient-derived muscle cells, along with positive changes in cell vitality (Figure 5). This provides strong evidence that this approach is both effective and safe at the cellular level, suggesting potential efficacy and safety for patients as well. Successful clinical translation of this therapeutic strategy could provide clinical benefits to patients with dysferlinopathy with mutations amenable to exon 27 skipping. In fact, its implementation could significantly impact patient care. These findings provide strong rationale for preclinical studies using suitable animal models to validate the efficacy, biodistribution, and safety of exon 27 skipping *in vivo* and potential clinical trials.

In parallel with exon skipping, some research groups have explored the design of adeno-associated virus (AAV)-mediated mini- and nano-dysferlin therapies by identifying and targeting redundant protein domains.[57] This approach is analogous to the microdystrophin therapy recently approved by the US Food and Drug Administration (FDA) for Duchenne muscular dystrophy.[58] However, the relationship between specific exon deletions and protein functionality in dysferlinopathies remains largely underexplored.[7] Furthermore, AAV-mediated gene therapies have been under scrutiny due to potential risks, including immune responses, organ toxicity, and insertional mutagenesis.[59] In contrast, exon-skipping therapies have not cast a spotlight on such serious risks associated with it, with four such therapies already receiving FDA approval and additional single and multi-exon-skipping therapies currently in development.[60–66] Despite the absence of approved genetic or other therapies specifically for dysferlinopathies, exon skipping presents a promising therapeutic strategy.[7] Our study provides substantial support for the development of exon-skipping therapies for dysferlinopathies, highlighting their potential efficacy and safety.

While the results we present here are promising, there are several limitations to our study. The *in vitro* nature of our experiments necessitates further validation *in vivo* to fully establish the efficacy, safety, and overall clinical potential of exon 27 skipping in a more complex biological context.[67,68] For instance, the *in vitro* persistence of the ASO treatment effect that we show may not fully capture the long-term *in vivo* outcomes due to inherent differences between cultured cells and physiological environments. Factors, for example, tissue-specific dynamics and protein turnover rates, can significantly impact the duration of protein expression *in vivo*.[69] Therefore, validating these results in animal models will be essential to assess long-term therapeutic outcomes, including biodistribution, persistence, and potential immune response of ASO treatments.[70] However, no established animal models are currently available for evaluating *DYSF* exon 27 skipping, which limits our capacity for comprehensive preclinical testing of this approach. Developing a humanized dysferlinopathy model carrying mutations analogous to human exon 26 deletion would allow for a comprehensive preclinical assessment of exon-skipping therapies and advance the translational potential of our approach.

In addition, while ASO treatment restored dysferlin function, it did not significantly alter myogenin or myomaker levels, and caveolin 3 expression remained lower than in healthy cells (Figure S4). These findings highlight the biological complexities of restoring muscle cell function in dysferlinopathies, suggesting that combining dysferlin restoration with approaches targeting its associated protein network may enhance therapeutic outcomes. Additionally, investigating interactions between myogenic fusion proteins and dysferlin could provide further insights into optimizing therapeutic strategies. The finding that both myogenin and myomaker were significantly elevated in patient-derived cells could be indicative of an intrinsic up-regulation as a compensatory response in dysferlin-deficient cells. In addition, future research should prioritize optimizing delivery methods for ASOs—such as nanoparticle carriers, cell-penetrating peptides, or small-molecule oligonucleotide activity enhancers—to enhance tissue specificity and reduce off-target effects, as efficient ASO delivery remains a significant challenge in the field.[71] These advancements are crucial for progressing toward clinical trials and ultimately offering a personalized therapeutic option for patients with dysferlinopathies. Furthermore, exploring the combination of exon skipping with complementary therapeutic strategies, such as small-molecule compensators for dysferlin deficiency, could further enhance treatment outcomes. Future research should also delve into personalized medicine approaches, tailoring ASOs to the specific mutational landscape of individual patients. This precision targeting could maximize therapeutic efficacy while minimizing off-target effects, paving the way for more individualized and effective treatment strategies for dysferlinopathy patients.

In conclusion, our study provides compelling evidence that ASO-mediated exon 27 skipping can effectively restore functional dysferlin protein in dysferlinopathy patient-derived muscle cells. This strategy not only offers a promising therapeutic avenue but also underscores the clinical feasibility of exon skipping as a personalized treatment approach. With continued research and clinical development, this approach holds significant potential to transform the management of dysferlinopathies and improve patient outcomes.

MATERIALS AND METHODS

Cell culture

Immortalized human muscle cells used in the study were kindly provided by the Institut de Myologie (Sorbonne Université-INSERM, Center de Recherche en Myologie, Paris) through Dr. Vincent Mouly. Two deidentified and anonymized cell lines were used: cell line 578

(cl.578) and KM155. The cl.578 (previously referred to as DYSF4) cell line is an immortalized myoblast line derived from the vastus lateralis of a patient in her late 20s, assigned female at birth, and diagnosed with LGMDR2.[72] This patient is of Arab descent and presented with a severe clinical phenotype that was more pronounced than typically observed in dysferlinopathy patients of this age. Histological examinations also revealed signs of glycogenosis in this patient. The KM155 cell line is an immortalized myoblast line isolated from the right semitendinosus of a 25-year-old healthy male individual. Experiments using human cells in this study were performed with approval from the Human Research Ethics Boards of the University of Alberta, Canada.

Both cell lines were grown in Dulbecco's Modified Eagle Medium:Nutrient Mixture F-12 containing HEPES (DMEM/F-12, HEPES; Gibco, Grand Island, NY), supplemented with 20% fetal bovine serum (Gibco), 1 vial of skeletal muscle growth supplement mix (PromoCell GmbH, Heidelberg, Germany), and 0.5% penicillin-streptomycin (10,000 U/mL; Gibco). These myoblasts were seeded into collagen type 1-coated 12-well plates (Corning Biocoat, Horsham, PA) at a density of 0.50×10^5 cells/cm^2. To induce differentiation into myotubes, the growth medium was replaced with differentiation medium composed of DMEM/F12, HEPES containing 2% equine serum (Cytiva, South Logan, UT), 1.0 μL/mL insulin-transferrin-selenium (Gibco), and 0.5% penicillin-streptomycin. The cells were maintained in this differentiation medium for 7 days. All cells were maintained at 37°C in a humidified atmosphere with 5% CO_2 until they were used for experiments.

ASO design, synthesis, and transfection

ASO sequences targeting *DYSF* exon 27 were designed using a self-developed *in silico* tool capable of estimating expected exon-skipping efficiency. The top three ASOs with the highest predicted exon-skipping ability and meeting technical criteria for synthesis (e.g., GC content, melting temperature [T_m], self-complementarity) were commercially synthesized by Gene Tools (Philomath, OR) using PMO chemistry (Figure 2A).

The synthesized ASOs were then transfected into ∼70% confluent cells at a 10.0-μM dose using 6.0 μM EndoPorter (Gene Tools) transfection reagent, as described previously.[73] A random control ASO (25-N; Gene Tools) was used for mock treatment, while non-treated samples received an equivalent volume of phosphate-buffered saline (PBS; Gibco) instead of ASO and/or EndoPorter solutions. The cells were maintained in the treatment media at 37°C in a humidified atmosphere with 5% CO_2 until they were used for downstream analysis.

DNA extraction and Sanger sequencing

Genomic DNA was extracted from cells using the Qiagen Blood & Cell Culture DNA Mini Kit (Qiagen, Hilden, Germany), following the manufacturer's guidelines. The extracted DNA, along with negative controls, was subjected to PCR amplification using GoTaq Green Master Mix (Promega, Madison, WI) in a SimpliAmp Thermal Cycler (Applied Biosystems, Singapore). Primers used for PCR amplification are listed in Table 1. PCR products (3.0, 5.0, or 10.0 μL) and either a 100-bp (Promega or New England Biolabs, Ipswich, MA) or a 1-kbp Plus (O'GeneRuler, Vilnius, Lithuania) DNA ladder were electrophoresed on 1.5% agarose gels (Invitrogen, Carlsbad, CA) and visualized using GelRed Nucleic Acid Stain (EMD Millipore, Temecula, CA) on a ChemiDoc Imaging System (Bio-Rad, Hercules, CA). Bands of interest were excised and purified using the PureLink Quick Gel Extraction Kit (Invitrogen). The purified PCR products were sequenced via Sanger sequencing at the University of Alberta's molecular biology core facility using the same primers used for amplification.

RNA extraction, RT-PCR, evaluation of exon-skipping efficiency, and Sanger sequencing

Total RNA was extracted from cells using a standard TRIzol-based method (Invitrogen) following the manufacturer's instructions with slight modifications, as described previously.[73] From this, 1,400 ng total RNA was used for cDNA synthesis using the SuperScript IV One-Step RT-PCR System (Invitrogen), as directed by the manufacturer, with 0.5 μg of oligo$(dT)_{12\text{-}18}$ (Invitrogen) as the primer in a final volume of 20 μL. A reaction containing nuclease-free water instead of RNA served as a negative control.

The synthesized cDNA was used as a template for RT-PCR in an Eppendorf Mastercycler Nexus Thermal Cycler (Eppendorf AG, Hamburg, Germany). Primers are listed in Table 1. PCR was performed with 4.0 μL cDNA or negative control using GoTaq Green Master Mix (Promega). To detect skipping, a forward exon 24 primer and a reverse exon 29 primer were used at final concentrations of 0.25 μM. The PCR program was (1) initial denaturation at 95°C for 2 min; (2) 35 or 40 cycles of denaturation at 95°C for 30 s, annealing at 56°C for 30 s, and extension at 72°C for 45 s; (3) final extension at 72°C for 5 min; and (4) hold at 4°C indefinitely. PCR products (3.0, 5.0, or 10.0 μL) and a 100 bp (Promega or New England Biolabs) or 100 bp Plus (GeneRuler, Thermo Scientific) were run on 1.5% agarose gels (Invitrogen) and visualized using GelRed Nucleic Acid Stain (EMD Millipore) on a ChemiDoc Imaging System (Bio-Rad). Band intensities were quantified using Image Lab 6.0.1 (Bio-Rad). Exon-skipping efficiency was calculated as the percentage of the skipped band intensity relative to the total intensity of the native, intermediate, and skipped bands.[73] To confirm the identities of each band of interest, Sanger sequencing was performed at the University of Alberta's molecular biology core facility using the same RT-PCR primers.

Protein extraction, quantification, and immunoblotting

We extracted proteins from cells using radioimmunoprecipitation assay buffer (Thermo Scientific) supplemented with cOmplete, Mini, EDTA-free protease inhibitor cocktail (Roche, Mannheim, Germany), as described previously. Proteins were quantified using the Pierce BCA Protein Assay Kit (Thermo Scientific) following the manufacturer's guidelines. The proteins were then subjected to immunoblotting according to our previously described protocol, with slight modifications.

For immunoblotting, a total of 1.5 or 5.0 or 12 μg of each protein sample was mixed with NuPAGE LDS Sample Buffer (Invitrogen; 1× final concentration) and NuPAGE Sample Reducing Agent

Table 1. Primers used for Sanger sequencing and RT-PCR

S. No.	Primer	Sequence (5′→3′)
Sanger sequencing primers for mutation analysis		
1	hDYSF_gDNA_F1	GGC CCT CCA GTA TGA GAA CG
2	hDYSF_gDNA_R1	CTG GGA GAG TTC AGC GGA AG
3	hGAPDH_gDNA_F1	TCC CTG AGC TGA ACG GGA AG
4	hGAPDH_gDNA_R1	GGA GGA GTG GGT GTC GCT GT
RT-PCR primers for skip efficiency analysis and Sanger sequencing of the RT-PCR products		
5	hDYSF_∇26/27_F1	GTG GGA AGC TAC AGA CAA TCT T
6	hDYSF_∇26/27_R1	CGG TGT GTG TAG TAC ATC TTC TC
7	hDYSF_∇26/27_F2	GTG GCA AGA ATT GTG GGA AG
8	hDYSF_∇26/27_R2	GGG ATG GTG ATG CTA TAC TCC
9	hGAPDH_cDNA_F1	CTT AGC ACC CCT GGC CAA G
10	hGAPDH_cDNA_R1	GTC AAA GGT GGA GGA GTG GG

(Invitrogen; 1× final concentration), then heated at 70°C for 10 min. Protein samples (1.5, 5.0, or 12 μg) were loaded onto pre-cast NuPAGE 3%–8% Tris-Acetate Midi gels (Invitrogen) for SDS-PAGE and run at 150 V for 70 min (dysferlin and α-tubulin) or 120 min (myogenin, myomaker, caveolin 3, and α-tubulin). Proteins were then transferred onto a polyvinylidene fluoride membrane (Millipore, Tullagreen, Ireland) using a semi-dry blotting system at 20 V for 70 min. Membranes were blocked in a solution of PBS containing 0.05% Tween 20 (PBS-T) and 5% skim milk while shaking. After blocking, the membranes were cut and incubated with one of the following primary antibodies overnight at 4°C in blocking solution: (1) dysferlin: NCL hamlet monoclonal antibody (Leica Biosystems, Wetzlar, Germany; 1:4,000), (2) α-tubulin: α-tubulin ab7291 antibody (Abcam, Cambridge, UK; 1:4,000), (3) myogenin: myogenin monoclonal antibody (clone: F5D, Invitrogen; 1:4,000), (4) caveolin 3: mouse anti-human caveolin 3 monoclonal antibody (MAB6706, R&D Systems, Minneapolis, MN; 1:4,000), and (5) myomaker: anti-TMEM8C antibody (ab188300, Abcam; 1:4,000). The membrane sections were then incubated with the following horseradish peroxidase (HRP)-conjugated secondary antibodies for 1 h at room temperature in PBS-T: (1) dysferlin and α-tubulin: goat anti-mouse immunoglobulin G (IgG) (H + L) secondary antibody (Invitrogen; 1:8,000), (2) myogenin: goat anti-mouse IgG (H + L) superclonal recombinant secondary antibody, HRP (A28177, Thermo Fisher Scientific; 1:8,000), (3) caveolin 3: goat anti-mouse IgG secondary antibody (Invitrogen; 1:8,000), and (4) myomaker: goat anti-rabbit IgG (H + L) (Invitrogen; 1:8,000). Membranes were washed in PBS-T and detected using ECL Select Detection Reagent (GE Healthcare, Little Chalfont, UK). Immunoblot bands were visualized using the ChemiDoc Imaging System (Bio-Rad), and densitometric quantification was performed using ImageLab 6.0.1 (Bio-Rad).

Laser wounding assay

Healthy and patient-derived myoblasts were seeded at a density of 0.50×10^5 cells/cm^2 into collagen type 1-coated 35-mm plates (MatTek, Ashland, MD) and treated as described above. The myoblast plasma membranes were then subjected to laser-induced injury using two-photon laser microscopy, following a previously described method with slight modifications.[73] The cells were prepared for two-photon laser-mediated wounding by rinsing once with Tyrode's salts solution (TriBioScience, Sunnyvale, CA) and then adding 1 mL Tyrode's salts containing 2.5 mM FM4-64 dye (Molecular Probes, Eugene, OR). A total of 27–30 cells per treatment group were wounded using a Zeiss LSM 710 inverted confocal laser scanning microscope and Zeiss ZEN software. A 0.2 × 2-μm target was placed at the edge of the cell membrane. A 5-min time series of sequential image scans was performed, with cells imaged every 5 s. Cells were ablated 25 s after the beginning of the time series using the two-photon laser set to 820 nm at 15% laser power with 10 iterations. Fluorescence values at sites of injury were quantified using Zeiss ZEN software. For each time point, relative fluorescence values were determined by subtracting the background value (mean of t = 0–25 s) and dividing the net increase in fluorescence by the background fluorescence value.

Immunostaining

Healthy and patient-derived myoblasts were seeded in collagen type 1-coated 24-well plates (Corning Biocoat, Horsham, PA) at a density of 0.50×10^5 cells/cm^2 and differentiated into myotubes for 7 days before treatment as described above. The cells were then fixed for 5 min with 4% freshly prepared paraformaldehyde (Sigma-Aldrich, St. Louis, MO), permeabilized for 5 min with 0.25% Triton X-100, and blocked with 1% normal goat serum (Sigma-Aldrich) diluted in PBS containing 0.1% Triton X-100 for 20 min. For immunostaining, anti-dystrophin antibody ab85302 (Abcam) was used as the primary antibody in combination with Alexa 488-conjugated anti-mouse IgG secondary antibodies (Invitrogen). Nuclei were counterstained with ProLong Gold Antifade Mountant with DAPI (4′,6-diamidino-2-phenylindole; Molecular Probes). Images were taken using a Zeiss Observer 5 fluorescence microscope with an attached AxioCam 202.

The MFI was calculated by dividing the number of myotube-residing nuclei (defined as cells with at least two nuclei sharing the same cytoplasm) by the total number of myotube-residing nuclei in an image, using the ImageJ tool (National Institutes of Health). The average MFI from three random fields of view was used for fusion index calculation for each replicate. Randomly selected myotubes were used for quantification; if fewer than 15 myotubes were present in each field of view, then all myotubes were considered for quantification. Fifteen wells with myotubes were measured for each treatment group.

Cell-level vitality, cytotoxicity, and apoptosis assessment

Cell vitality, cytotoxicity, and apoptosis were evaluated using the ApoTox-Glo Triplex Assay Kit (Promega) following the manufacturer's protocol. Briefly, healthy and patient-derived myoblasts were seeded at a density of 0.50×10^5 cells/cm^2 into collagen type 1-coated 96-well flat-bottom microplates (Corning Biocoat) and treated as described above. Twenty microliters of viability/cytotoxicity reagent containing glycyphenylalanyl-aminofluorocoumarin

(AFC) and bis-alanylalanyl-phenylalnyl-rhodamine 110 substrates was added for cell viability and cytotoxicity measurements, respectively. Plates were placed on an orbital shaker set at 300 rpm for 30 s and then incubated at 37°C for 40 min. Post-incubation, fluorescence was measured at 400 nm (excitation)/505 nm (emission) for viability and 485 nm (excitation)/520 nm (emission) for cytotoxicity. Viable cells show a decrease in AFC fluorescence, while dead cells show an increase. Thereafter, for apoptosis analysis, 100 μL of the Caspase-Glo 3/7 reagent was added to all wells. Plates were placed on an orbital shaker set at 300 rpm for 30 s and then incubated at room temperature for 40 min. Luminescence signals were measured using the SpectraMax M Series Multi-Mode Microplate Reader (Molecular Devices, San Jose, CA).

Statistical analysis

All statistical tests were performed using GraphPad Prism version 9.0.1 (GraphPad, San Diego, CA). Unpaired two-tailed one-way ANOVA with post-hoc Tukey's or Dunnett's multiple comparisons tests were conducted as appropriate. Analyses were performed at α levels of 0.05, 0.01, 0.001, and 0.0001 ($p = 0.05$, $p = 0.01$, $p = 0.001$, and $p = 0.0001$, respectively).

DATA AND CODE AVAILABILITY

The datasets generated and analyzed during the present study are available from the corresponding author upon reasonable request. Any additional information (e.g., raw sequencing data) required to interpret, verify, or extend the findings of this study can be obtained by contacting the corresponding author.

ACKNOWLEDGMENTS

We thank Dr. Vincent Mouly (Institut de Myologie, Sorbonne Université-INSERM, Center de Recherche en Myologie, Paris) for his assistance in supplying us with the dysferlinopathy patient-derived myoblasts. We also express our heartfelt gratitude to Dr. Simone Spuler (Charité Universitätsmedizin Berlin and Max Delbrück Center, Berlin) for sharing clinical information about the patient from whom the dysferlinopathy patient-derived myoblasts were obtained. Also, we wish to thank Dr. Kenji Rowel Quintana Lim (Washington University in St. Louis, St. Louis, MO) and Md. Nur Ahad Shah (University of Alberta, Edmonton, AB) for their intellectual support and generous assistance with the experiments. We thank Jarin Taslem Mourosi (the Catholic University of America, Washington, DC) for her assistance in preparing some of the figures using the BioRender web interface. T.Y. is supported by the University of Alberta Faculty of Medicine and Dentistry, the Friends of Garrett Cumming Research Chair Fund, the Henry M. Toupin Neurological Science Research Chair Fund, Muscular Dystrophy Canada, the Canada Foundation for Innovation, the Alberta Advanced Education and Technology, Canadian Institutes of Health Research, the Women and Children's Health Research Institute (WCHRI), and Alberta Innovates - Health Solutions. R.R.R. received the Alberta Innovates Summer Research Studentship award. S.A. is supported by scholarships from the Maternal and Child Health Program, the Alberta Innovates Graduate Student Scholarship, the WCHRI Graduate Studentship, the Andrew Stewart Memorial Graduate Prize, and the Alberta Graduate Excellence Scholarship.

AUTHOR CONTRIBUTIONS

Conceptualization, S.A. and T.Y.; design, S.A., J.J.A.L., and W.J.D.; funding acquisition, T.Y.; data curation, S.A. and U.S.H.; methodology, S.A., R.R.R., S.W., R.M., and T.Y.; investigation, S.A., R.R.R., and S.W.; formal analysis, S.A. and T.Y.; validation, S.A. and U.S.H.; visualization, S.A.; project administration, S.A., R.M., and T.Y.; supervision, R.M. and T.Y.; resources, S.A., V.M., and T.Y.; software, S.A., W.J.D., R.M., and T.Y.; writing – original draft, S.A.; writing – review & editing, S.A. and T.Y.

DECLARATION OF INTERESTS

T.Y. and R.M. are cofounders of OligomicsTx.

SUPPLEMENTAL INFORMATION

Supplemental information can be found online at https://doi.org/10.1016/j.omtn.2024.102443.

REFERENCES

1. Bashir, R., Britton, S., Strachan, T., Keers, S., Vafiadaki, E., Lako, M., Richard, I., Marchand, S., Bourg, N., Argov, Z., et al. (1998). A gene related to Caenorhabditis elegans spermatogenesis factor fer-1 is mutated in limb-girdle muscular dystrophy type 2B. Nat. Genet. *20*, 37–42. https://doi.org/10.1038/1689.

2. Liu, J., Aoki, M., Illa, I., Wu, C., Fardeau, M., Angelini, C., Serrano, C., Urtizberea, J.A., Hentati, F., Hamida, M.B., et al. (1998). Dysferlin, a novel skeletal muscle gene, is mutated in Miyoshi myopathy and limb girdle muscular dystrophy. Nat. Genet. *20*, 31–36. https://doi.org/10.1038/1682.

3. Liu, W., Pajusalu, S., Lake, N.J., Zhou, G., Ioannidis, N., Mittal, P., Johnson, N.E., Weihl, C.C., Williams, B.A., Albrecht, D.E., et al. (2019). Estimating prevalence for limb-girdle muscular dystrophy based on public sequencing databases. Genet. Med. *21*, 2512–2520. https://doi.org/10.1038/s41436-019-0544-8.

4. Theadom, A., Rodrigues, M., Roxburgh, R., Balalla, S., Higgins, C., Bhattacharjee, R., Jones, K., Krishnamurthi, R., and Feigin, V. (2014). Prevalence of muscular dystrophies: A systematic literature review. Neuroepidemiology *43*, 259–268. https://doi.org/10.1159/000369343.

5. Mah, J.K., Korngut, L., Fiest, K.M., Dykeman, J., Day, L.J., Pringsheim, T., and Jette, N. (2016). A Systematic Review and Meta-analysis on the Epidemiology of the Muscular Dystrophies. Can. J. Neurol. Sci. *43*, 163–177. https://doi.org/10.1017/cjn.2015.311.

6. Bardakov, S.N., Deev, R.V., Isaev, A.A., Khromov-Borisov, N.N., Kopylov, E.D., Savchuk, M.R., Pushkin, M.S., Presnyakov, E.V., Magomedova, R.M., Achmedova, P.G., et al. (2023). Genetic screening of an endemic mutation in the DYSF gene in an isolated, mountainous population in the Republic of Dagestan. Mol. Genet. Genomic Med. *11*, e2236. https://doi.org/10.1002/mgg3.2236.

7. Anwar, S., and Yokota, T. (2024). The Dysferlinopathies Conundrum: Clinical Spectra, Disease Mechanism and Genetic Approaches for Treatments. Biomolecules *14*, 256. https://doi.org/10.3390/biom14030256.

8. Aoki, M., Liu, J., Richard, I., Bashir, R., Britton, S., Keers, S.M., Oeltjen, J., Brown, H.E., Marchand, S., Bourg, N., et al. (2001). Genomic organization of the dysferlin gene and novel mutations in Miyoshi myopathy. Neurology *57*, 271–278. https://doi.org/10.1212/wnl.57.2.271.

9. Ivanova, A., Smirnikhina, S., and Lavrov, A. (2022). Dysferlinopathies: Clinical and genetic variability. Clin. Genet. *102*, 465–473. https://doi.org/10.1111/cge.14216.

10. Mahjneh, I., Bushby, K., Passos-Bueno, M.-R., Zatz, M., Nasher, L., Bashir, R., Strachan, T., and Marconi, G. (1996). The phenotype of chromosome 2P-linked limb-girdle muscular dystrophy. Neuromuscul. Disord. *6*, S7. https://doi.org/10.1016/0960-8966(96)88958-9.

11. Illa, I., Serrano-Munuera, C., Gallardo, E., Lasa, A., Rojas-García, R., Palmer, J., Gallano, P., Baiget, M., Matsuda, C., and Brown, R.H. (2001). Distal anterior compartment myopathy: A dysferlin mutation causing a new muscular dystrophy phenotype. Ann. Neurol. *49*, 130–134. https://doi.org/10.1002/1531-8249(200101)49:1<130::aid-ana22>3.3.co;2-s.

12. Galassi, G., Rowland, L.P., Hays, A.P., Hopkins, L.C., and DiMauro, S. (1987). High serum levels of creatine kinase: Asymptomatic prelude to distal myopathy. Muscle Nerve *10*, 346–350. https://doi.org/10.1002/mus.880100411.

13. Aoki, M., and Takahashi, T. (2021). Dysferlinopathy. In GeneReviews® [Internet], M.P. Adam, G.M. Mirzaa, and R.A. Pagon, eds. (University of Washington), p. NBK1303.

14. Guglieri, M., Magri, F., D'Angelo, M.G., Prelle, A., Morandi, L., Rodolico, C., Cagliani, R., Mora, M., Fortunato, F., Bordoni, A., et al. (2008). Clinical, molecular, and protein correlations in a large sample of genetically diagnosed Italian limb girdle muscular dystrophy patients. Hum. Mutat. *29*, 258–266. https://doi.org/10.1002/humu.20642.

15. Krahn, M., Béroud, C., Labelle, V., Nguyen, K., Bernard, R., Bassez, G., Figarella-Branger, D., Fernandez, C., Bouvenot, J., Richard, I., et al. (2009). Analysis of the DYSF mutational spectrum in a large cohort of patients. Hum. Mutat. *30*, E345–E375. https://doi.org/10.1002/humu.20910.

16. Xi, J., Blandin, G., Lu, J., Luo, S., Zhu, W., Béroud, C., Pécheux, C., Labelle, V., Lévy, N., Urtizberea, J.A., et al. (2014). Clinical heterogeneity and a high proportion of novel mutations in a chinese cohort of patients with dysferlinopathy. Neurol. India *62*, 635–639. https://doi.org/10.4103/0028-3886.149386.

17. Nguyen, K., Bassez, G., Krahn, M., Bernard, R., Laforêt, P., Labelle, V., Urtizberea, J.A., Figarella-Branger, D., Romero, N., Attarian, S., et al. (2007). Phenotypic study in 40 patients with dysferlin gene mutations: High frequency of atypical phenotypes. Arch. Neurol. *64*, 1176–1182. https://doi.org/10.1001/archneur.64.8.1176.

18. Nguyen, K., Bassez, G., Bernard, R., Krahn, M., Labelle, V., Figarella-Branger, D., Pouget, J., Hammouda, E.H., Béroud, C., Urtizberea, A., et al. (2005). Dysferlin mutations in LGMD2B, Miyoshi myopathy, and atypical dysferlinopathies. Hum. Mutat. *26*, 165. https://doi.org/10.1002/humu.9355.

19. Bansal, D., Miyake, K., Vogel, S.S., Groh, S., Chen, C.C., Williamson, R., McNeil, P.L., and Campbell, K.P. (2003). Defective membrane repair in dysferlin-deficient muscular dystrophy. Nature *423*, 168–172. https://doi.org/10.1038/nature01573.

20. Bansal, D., and Campbell, K.P. (2004). Dysferlin and the plasma membrane repair in muscular dystrophy. Trends Cell Biol. *14*, 206–213. https://doi.org/10.1016/j.tcb.2004.03.001.

21. Glover, L., and Brown, R.H. (2007). Dysferlin in Membrane Trafficking and Patch Repair. Traffic *8*, 785–794. https://doi.org/10.1111/j.1600-0854.2007.00573.x.

22. Kawahara, G., Serafini, P.R., Myers, J.A., Alexander, M.S., and Kunkel, L.M. (2011). Characterization of zebrafish dysferlin by morpholino knockdown. Biochem. Biophys. Res. Commun. *413*, 358–363. https://doi.org/10.1016/j.bbrc.2011.08.105.

23. Kerr, J.P., Ziman, A.P., Mueller, A.L., Muriel, J.M., Kleinhans-Welte, E., Gumerson, J.D., Vogel, S.S., Ward, C.W., Roche, J.A., and Bloch, R.J. (2013). Dysferlin stabilizes stress-induced Ca2+ signaling in the transverse tubule membrane. Proc. Natl. Acad. Sci. USA *110*, 20831–20836. https://doi.org/10.1073/pnas.1307960110.

24. Klinge, L., Laval, S., Keers, S., Haldane, F., Straub, V., Barresi, R., and Bushby, K. (2007). From T-tubule to sarcolemma: damage-induced dysferlin translocation in early myogenesis. Faseb. J. *21*, 1768–1776. https://doi.org/10.1096/fj.06-7659com.

25. Hofhuis, J., Bersch, K., Büssenschütt, R., Drzymalski, M., Liebetanz, D., Nikolaev, V.O., Wagner, S., Maier, L.S., Gärtner, J., Klinge, L., and Thoms, S. (2017). Dysferlin mediates membrane tubulation and links T-tubule biogenesis to muscular dystrophy. J. Cell Sci. *130*, 841–852. https://doi.org/10.1242/jcs.198861.

26. Anderson, L.V., Davison, K., Moss, J.A., Young, C., Cullen, M.J., Walsh, J., Johnson, M.A., Bashir, R., Britton, S., Keers, S., et al. (1999). Dysferlin is a plasma membrane protein and is expressed early in human development. Hum. Mol. Genet. *8*, 855–861. https://doi.org/10.1093/hmg/8.5.855.

27. BioGPS GeneAtlas U133A, gcrma. biogps.org, Probeset: 218660_at. http://biogps.org/#goto=genereport&id=8291.

28. Lek, A., Evesson, F.J., Sutton, R.B., North, K.N., and Cooper, S.T. (2012). Ferlins: Regulators of Vesicle Fusion for Auditory Neurotransmission, Receptor Trafficking and Membrane Repair. Traffic *13*, 185–194. https://doi.org/10.1111/j.1600-0854.2011.01267.x.

29. Leung, C., Yu, C., Lin, M.I., Tognon, C., and Bernatchez, P. (2013). Expression of myoferlin in human and murine carcinoma tumors: Role in membrane repair, cell proliferation, and tumorigenesis. Am. J. Pathol. *182*, 1900–1909. https://doi.org/10.1016/j.ajpath.2013.01.041.

30. Cárdenas, A.M., González-Jamett, A.M., Cea, L.A., Bevilacqua, J.A., and Caviedes, P. (2016). Dysferlin function in skeletal muscle: Possible pathological mechanisms and therapeutical targets in dysferlinopathies. Exp. Neurol. *283*, 246–254. https://doi.org/10.1016/j.expneurol.2016.06.026.

31. Sula, A., Cole, A.R., Yeats, C., Orengo, C., and Keep, N.H. (2014). Crystal structures of the human Dysferlin inner DysF domain. BMC Struct. Biol. *14*, 3. https://doi.org/10.1186/1472-6807-14-3.

32. Harsini, F.M., Chebrolu, S., Fuson, K.L., White, M.A., Rice, A.M., and Sutton, R.B. (2018). FerA is a Membrane-Associating Four-Helix Bundle Domain in the Ferlin Family of Membrane-Fusion Proteins. Sci. Rep. *8*, 10949. https://doi.org/10.1038/s41598-018-29184-1.

33. Harsini, F.M., Bui, A.A., Rice, A.M., Chebrolu, S., Fuson, K.L., Turtoi, A., Bradberry, M., Chapman, E.R., and Sutton, R.B. (2019). Structural Basis for the Distinct Membrane Binding Activity of the Homologous C2A Domains of Myoferlin and Dysferlin. J. Mol. Biol. *431*, 2112–2126. https://doi.org/10.1016/j.jmb.2019.04.006.

34. Patel, P., Harris, R., Geddes, S.M., Strehle, E.-M., Watson, J.D., Bashir, R., Bushby, K., Driscoll, P.C., and Keep, N.H. (2008). Solution Structure of the Inner DysF Domain of Myoferlin and Implications for Limb Girdle Muscular Dystrophy Type 2B. J. Mol. Biol. *379*, 981–990. https://doi.org/10.1016/j.jmb.2008.04.046.

35. Ponting, C.P., Mott, R., Bork, P., and Copley, R.R. (2001). Novel Protein Domains and Repeats in Drosophila melanogaster : Insights into Structure, Function, and Evolution. Genome Res. *11*, 1996–2008. https://doi.org/10.1101/gr.198701.

36. Sinnreich, M., Therrien, C., and Karpati, G. (2006). Lariat branch point mutation in the dysferlin gene with mild limb-girdle muscular dystrophy. Neurology *66*, 1114–1116. https://doi.org/10.1212/01.wnl.0000204358.89303.81.

37. Veltrop, M., and Aartsma-Rus, A. (2014). Antisense-mediated exon skipping: Taking advantage of a trick from Mother Nature to treat rare genetic diseases. Exp. Cell Res. *325*, 50–55. https://doi.org/10.1016/j.yexcr.2014.01.026.

38. Barthélémy, F., Blouin, C., Wein, N., Mouly, V., Courrier, S., Dionnet, E., Kergourlay, V., Mathieu, Y., Garcia, L., Butler-Browne, G., et al. (2015). Exon 32 Skipping of Dysferlin Rescues Membrane Repair in Patients' Cells. J. Neuromuscul. Dis. *2*, 281–290. https://doi.org/10.3233/JND-150109.

39. Aartsma-Rus, A., Singh, K.H.K., Fokkema, I.F.A.C., Ginjaar, I.B., van Ommen, G.-J., den Dunnen, J.T., and van der Maarel, S.M. (2010). Therapeutic exon skipping for dysferlinopathies? Eur. J. Hum. Genet. *18*, 889–894. https://doi.org/10.1038/ejhg.2010.4.

40. Verwey, N., Gazzoli, I., Krause, S., Mamchaoui, K., Mouly, V., and Aartsma-Rus, A. (2020). Antisense-Mediated Skipping of Dysferlin Exons in Control and Dysferlinopathy Patient-Derived Cells. Nucleic Acid Therapeut. *30*, 71–79. https://doi.org/10.1089/nat.2019.0788.

41. Lee, J.J.A., Maruyama, R., Duddy, W., Sakurai, H., and Yokota, T. (2018). Identification of Novel Antisense-Mediated Exon Skipping Targets in DYSF for Therapeutic Treatment of Dysferlinopathy. Mol. Ther. Nucleic Acids *13*, 596–604. https://doi.org/10.1016/j.omtn.2018.10.004.

42. Dominov, J.A., Uyan, Ö., Sapp, P.C., McKenna-Yasek, D., Nallamilli, B.R.R., Hegde, M., and Brown, R.H. (2014). A novel dysferlin mutant pseudoexon bypassed with antisense oligonucleotides. Ann. Clin. Transl. Neurol. *1*, 703–720. https://doi.org/10.1002/acn3.96.

43. Izumi, R., Takahashi, T., Suzuki, N., Niihori, T., Ono, H., Nakamura, N., Katada, S., Kato, M., Warita, H., Tateyama, M., et al. (2020). The genetic profile of dysferlinopathy in a cohort of 209 cases: Genotype–phenotype relationship and a hotspot on the inner DysF domain. Hum. Mutat. *41*, 1540–1554. https://doi.org/10.1002/humu.24036.

44. Echigoya, Y., Mouly, V., Garcia, L., Yokota, T., and Duddy, W. (2015). In Silico Screening Based on Predictive Algorithms as a Design Tool for Exon Skipping Oligonucleotides in Duchenne Muscular Dystrophy. PLoS One *10*, e0120058. https://doi.org/10.1371/journal.pone.0120058.

45. Chiba, S., Lim, K.R.Q., Sheri, N., Anwar, S., Erkut, E., Shah, M.N.A., Aslesh, T., Woo, S., Sheikh, O., Maruyama, R., et al. (2021). eSkip-Finder: a machine learning-based web application and database to identify the optimal sequences of antisense oligonucleotides for exon skipping. Nucleic Acids Res. *49*, W193–W198. https://doi.org/10.1093/nar/gkab442.

46. Defour, A., Van der Meulen, J.H., Bhat, R., Bigot, A., Bashir, R., Nagaraju, K., and Jaiswal, J.K. (2014). Dysferlin regulates cell membrane repair by facilitating injury-triggered acid sphingomyelinase secretion. Cell Death Dis. *5*, e1306. https://doi.org/10.1038/cddis.2014.272.

47. Quinn, C.J., Cartwright, E.J., Trafford, A.W., and Dibb, K.M. (2024). On the role of dysferlin in striated muscle: membrane repair, t-tubules and Ca 2+ handling. J. Physiol. *602*, 1893–1910. https://doi.org/10.1113/JP285103.

48. Jimenez, A.J., Maiuri, P., Lafaurie-Janvore, J., Perez, F., and Piel, M. (2015). Laser induced wounding of the plasma membrane and methods to study the repair process. In Methods Cell Biol., *125*, E.K. Paluch, ed. (Academic Press (Elsevier), pp. 391–408. https://doi.org/10.1016/bs.mcb.2014.11.007.

49. Lee, J.J.A., Maruyama, R., Sakurai, H., and Yokota, T. (2018). Cell Membrane Repair Assay Using a Two-photon Laser Microscope. J. Vis. Exp. *131*, 56999. https://doi.org/10.3791/56999.

50. de Luna, N., Gallardo, E., Soriano, M., Dominguez-Perles, R., de la Torre, C., Rojas-García, R., García-Verdugo, J.M., and Illa, I. (2006). Absence of Dysferlin Alters

Myogenin Expression and Delays Human Muscle Differentiation "in Vitro.". J. Biol. Chem. *281*, 17092–17098. https://doi.org/10.1074/jbc.M601885200.

51. Cohen, T.V., Cohen, J.E., and Partridge, T.A. (2012). Myogenesis in dysferlin-deficient myoblasts is inhibited by an intrinsic inflammatory response. Neuromuscul. Disord. *22*, 648–658. https://doi.org/10.1016/j.nmd.2012.03.002.
52. Gordon, J.L., Brown, M.A., and Reynolds, M.M. (2018). Cell-Based Methods for Determination of Efficacy for Candidate Therapeutics in the Clinical Management of Cancer. Diseases *6*, 85. https://doi.org/10.3390/diseases6040085.
53. Khalef, L., Lydia, R., Filicia, K., and Moussa, B. (2024). Cell viability and cytotoxicity assays: Biochemical elements and cellular compartments. Cell Biochem. Funct. *42*, e4007. https://doi.org/10.1002/cbf.4007.
54. Wein, N., Avril, A., Bartoli, M., Beley, C., Chaouch, S., Laforêt, P., Behin, A., Butler-Browne, G., Mouly, V., Krahn, M., et al. (2010). Efficient bypass of mutations in dysferlin deficient patient cells by antisense-induced exon skipping. Hum. Mutat. *31*, 136–142. https://doi.org/10.1002/humu.21160.
55. Echigoya, Y., Mouly, V., Garcia, L., Yokota, T., and Duddy, W. (2015). In Silico Screening Based on Predictive Algorithms as a Design Tool for Exon Skipping Oligonucleotides in Duchenne Muscular Dystrophy. PLoS One *10*, e0120058. https://doi.org/10.1371/journal.pone.0120058.
56. Izumi, R., Niihori, T., Takahashi, T., Suzuki, N., Tateyama, M., Watanabe, C., Sugie, K., Nakanishi, H., Sobue, G., Kato, M., et al. (2015). Genetic profile for suspected dysferlinopathy identified by targeted next-generation sequencing. Neurol. Genet. *1*, e36. https://doi.org/10.1212/NXG.0000000000000036.
57. Llanga, T., Nagy, N., Conatser, L., Dial, C., Sutton, R.B., and Hirsch, M.L. (2017). Structure-Based Designed Nano-Dysferlin Significantly Improves Dysferlinopathy in BLA/J Mice. Mol. Ther. *25*, 2150–2162. https://doi.org/10.1016/j.ymthe.2017.05.013.
58. Hoy, S.M. (2023). Delandistrogene Moxeparvovec: First Approval. Drugs *83*, 1323–1329. https://doi.org/10.1007/s40265-023-01929-x.
59. Wilton-Clark, H., and Yokota, T. (2023). Safety concerns surrounding AAV and CRISPR therapies in neuromuscular treatment. Méd. *4*, 855–856. https://doi.org/10.1016/j.medj.2023.11.008.
60. Lim, K.R.Q., Maruyama, R., and Yokota, T. (2017). Eteplirsen in the treatment of Duchenne muscular dystrophy. Drug Des. Dev. Ther. *11*, 533–545. https://doi.org/10.2147/DDDT.S97635.
61. Anwar, S., and Yokota, T. (2020). Golodirsen for Duchenne muscular dystrophy. Drugs Today *56*, 491–504. https://doi.org/10.1358/dot.2020.56.8.3159186.
62. Roshmi, R.R., and Yokota, T. (2019). Viltolarsen for the treatment of Duchenne muscular dystrophy. Drugs Today *55*, 627–639. https://doi.org/10.1358/dot.2019.55.10.3045038.
63. Wilton-Clark, H., and Yokota, T. (2021). Casimersen for Duchenne muscular dystrophy. Drugs Today *57*, 707–717. https://doi.org/10.1358/dot.2021.57.12.3352740.
64. Tang, A., and Yokota, T. (2024). Duchenne muscular dystrophy: promising early-stage clinical trials to watch. Expet Opin. Invest. Drugs *33*, 201–217. https://doi.org/10.1080/13543784.2024.2313105.
65. Lim, K.R.Q., Echigoya, Y., Nagata, T., Kuraoka, M., Kobayashi, M., Aoki, Y., Partridge, T., Maruyama, R., Takeda, S., and Yokota, T. (2019). Efficacy of Multi-exon Skipping Treatment in Duchenne Muscular Dystrophy Dog Model Neonates. Mol. Ther. *27*, 76–86. https://doi.org/10.1016/j.ymthe.2018.10.011.
66. Lim, K.R.Q., Woo, S., Melo, D., Huang, Y., Dzierlega, K., Shah, M.N.A., Aslesh, T., Roshmi, R.R., Echigoya, Y., Maruyama, R., et al. (2022). Development of DG9 peptide-conjugated single- and multi-exon skipping therapies for the treatment of Duchenne muscular dystrophy. Proc. Natl. Acad. Sci. USA *119*, e2112546119. https://doi.org/10.1073/pnas.2112546119.
67. Domínguez-Oliva, A., Hernández-Ávalos, I., Martínez-Burnes, J., Olmos-Hernández, A., Verduzco-Mendoza, A., and Mota-Rojas, D. (2023). The Importance of Animal Models in Biomedical Research: Current Insights and Applications. Animals *13*, 1223. https://doi.org/10.3390/ani13071223.
68. Yokota, T., Duddy, W., and Partridge, T. (2007). Optimizing exon skipping therapies for DMD. Acta Myol. *26*, 179–184.
69. Kilanowska, A., and Studzińska, S. (2020). In vivo and in vitro studies of antisense oligonucleotides – a review. RSC Adv. *10*, 34501–34516. https://doi.org/10.1039/D0RA04978F.
70. Egorova, Tatiana V., Galkin, Ivan I., Ivanova, Yulia V., and Polikarpova, Anna V. (2022). Duchenne Muscular Dystrophy Animal Models. In Preclinical Animal Modeling in Medicine (IntechOpen). https://doi.org/10.5772/intechopen.96738.
71. Anwar, S., Mir, F., and Yokota, T. (2023). Enhancing the Effectiveness of Oligonucleotide Therapeutics Using Cell-Penetrating Peptide Conjugation, Chemical Modification, and Carrier-Based Delivery Strategies. Pharmaceutics *15*, 1130. https://doi.org/10.3390/pharmaceutics15041130.
72. Philippi, S., Bigot, A., Marg, A., Mouly, V., Spuler, S., and Zacharias, U. (2012). Dysferlin-deficient immortalized human myoblasts and myotubes as a useful tool to study dysferlinopathy. PLoS Curr. *4*, RRN1298. https://doi.org/10.1371/currents.RRN1298.
73. Anwar, S., and Yokota, T. (2023). Morpholino-Mediated Exons 28–29 Skipping of Dysferlin and Characterization of Multiexon-skipped Dysferlin using RT-PCR, Immunoblotting, and Membrane Wounding Assay. In Muscular Dystrophy Therapeutics. Methods Mol. Biol. *2587*, 183–196. https://doi.org/10.1007/978-1-0716-2772-3_11.